Radiological Physics and Technology (2019) 12:46–54
https://doi.org/10.1007/s12194-018-0490-1

Early detection of elevated lactate levels in a mitochondrial disease model using chemical exchange saturation transfer (CEST) and magnetic resonance spectroscopy (MRS) at 7T-MRI

Shigeyoshi Saito[1,2] · Yusuke Takahashi[3] · Akiko Ohki[2] · Yasunori Shintani[4] · Takahiro Higuchi[2,5,6]

Received: 5 October 2018 / Revised: 16 November 2018 / Accepted: 17 November 2018 / Published online: 22 November 2018

Abstract

This study aimed to use chemical exchange saturation transfer (CEST) and magnetic resonance spectroscopy (MRS) at 7T-MRI for early detection of intracerebral lactate in a mitochondrial disease model without brain lesions. We considered *Ndufs4*-knockout (KO) mice as Leigh syndrome models and wild-type (WT) mice as control mice. Brain MRI and ^{1}H-MRS were performed. T_2WI data acquired with the Rapid Acquisition with Refocused Echoes (RARE) sequence were used for evaluation of brain lesions. CEST imaging of mice brains was performed using RARE with a magnetization transfer (MT) pulse. The MT ratio (MTR) asymmetry curves and five MTR asymmetry maps at 0.5, 1.0, 2.0, 3.0, and 3.5 ppm were calculated using these CEST images. Metabolite concentrations were measured by MRS. T_2WI MRI revealed no obvious abnormal findings in KO and WT mice brains at 6 weeks of age. The MTR asymmetry maps at 0.5 ppm, 1.0 ppm, and 2.0 ppm of the KO mice were higher than those of the control mice. Brain ^{1}H MRS revealed a significant increase in lactate levels in all KO mice in comparison with those in the control mice. Additionally, creatine levels in the KO mice were slightly higher than those in the control mice. The levels of the other four metabolites—mIns, NAA + NAAG, GPC + PCh, and Glu + Gln—did not change significantly. We propose that CEST imaging can be used as a biomarker of intracerebral elevated lactate levels in mitochondrial disease.

Keywords Mitochondrial disease · Chemical exchange saturation transfer · Magnetic resonance spectroscopy · Magnetic resonance imaging

Abbreviations

ATP	Adenosine triphosphate
CEST	Chemical exchange saturation transfer
CSI	Chemical shift imaging
FASTMAP	Fast automated shimming technique by mapping along projections
KO	Knock out
mM	Mmol/L
MTR	Magnetization transfer ratio
MR	Magnetic resonance
MRI	Magnetic resonance imaging
NOE	Nuclear overhauser enhancements
PRESS	Point resolved spectroscopy
RARE	Rapid acquisition with refocused echoes
SD	Standard deviation
TE	Echo time
TR	Repetition time
T_2WI	T_2-weighted images
VAPOR	Variable power RF pulses with optimized relaxation delays
WT	Wild type
WASSR	Water saturation shift referencing
^{1}H MRS	Proton magnetic resonance spectroscopy

✉ Shigeyoshi Saito
saito@sahs.med.osaka-u.ac.jp

[1] Division of Health Sciences, Department of Medical Physics and Engineering, Osaka University Graduate School of Medicine, Suita, Osaka 560-0871, Japan

[2] Department of Biomedical Imaging, National Cardiovascular and Cerebral Research Center, Suita, Osaka 565-8565, Japan

[3] Department of Cardiovascular Medicine, Osaka University Graduate School of Medicine, Suita, Osaka 565-0871, Japan

[4] Department of Medical Biochemistry, Osaka University Graduate School of Frontier Bioscience, Suita, Osaka 565-0871, Japan

[5] Comprehensive Heart Failure Center, University of Wuerzburg, 97078 Wuerzburg, Germany

[6] Department of Nuclear Medicine, University of Wuerzburg, 97078 Wuerzburg, Germany

1 Introduction

Mitochondrial diseases are a group of disorders caused by dysfunctional mitochondria, the organelles that generate energy for the cell [1]. The mitochondria play a dominant role in the production of adenosine triphosphate (ATP), as reflected by the large number of proteins in the inner membrane. Therefore, mitochondrial dysfunction leads to ATP depletion and redox imbalance [1–3]. Many patients with mitochondrial disease have consistently elevated lactic acid levels.

A mitochondrial disease that causes prominent muscular problems is called a mitochondrial myopathy, while a mitochondrial disease that causes both prominent muscular and neurological problems is called a mitochondrial encephalomyopathy. Leigh syndrome is one of the most severe mitochondrial diseases and results in death within 2 years after birth [4]. Because of these effects, mitochondrial diseases are life-threatening, progressive, and often associated with premature death [5–7]. Therefore, developing feasible animal models is important, not only to better understand the pathophysiology of mitochondrial diseases, but also to develop effective therapies [8].

Magnetic resonance spectroscopy (MRS) has previously been shown to help detect the abnormal accumulation of lactate in brain parenchyma and cerebral blood flow in association with mitochondrial disorders [9]. Previous studies have shown a significant intracerebral lactate peak in patients with mitochondrial disease [10–12]. However, there have been no evaluations of in vivo methods in animal models of mitochondrial disease.

Chemical exchange transfer (CEST) is a new imaging technique introduced in 2000 [13]. It is based on the magnetization transfer between bulk-water protons and exchangeable protons such as amide protons (–NH), amine protons ($–NH_2$), and hydroxyl protons (–OH), whose chemical shifts are 3.5 ppm, 1.8–3.0 ppm, and 0.5–1.5 ppm, respectively [14]. To evaluate animal models, some compounds containing these endogenous protons such as glutamate [15], creatine [16, 17], lactate [18], and other metabolites have been imaged using CEST. Brosse et al. demonstrated the feasibility of imaging lactate with CEST in lactate phantoms under physiological conditions in a mouse model of lymphoma tumors and in the skeletal muscle of healthy human subjects pre- and post-exercise [18]. In addition, they reported that creatine CEST can noninvasively detect changes in muscle creatine content and oxidative phosphorylation capacity in individuals with mitochondrial disorders [19]. However, there are no reports of intracerebral lactate evaluation in animal models of mitochondrial disease using CEST imaging.

Since CEST has the potential to be a sensitive tool to detect intracerebral lactate of some diseases and to clarify related physiological functions, the purpose of this study was to detect intracerebral lactate in a mitochondrial disease model using CEST and MRS at 7T-MRI.

2 Methods

2.1 Animal preparation

All animal procedures were approved by the Institutional Animal Care and Use Committee of our institute. The animals were fed sterile food and water, housed in sterile cages, and placed in rooms with a controlled temperature and humidity. Mice heterozygous for the deleted *Ndufs4* allele were obtained from Jackson laboratories (Bar Harbor, Maine, USA). We considered only the homozygous *Ndufs4*-knockout (KO) mice as Leigh syndrome mouse models (KO mice) and wild-type (WT) mice as controls [20–23]. Pups were genotyped at 28 days of age. Leigh syndrome is a severe neurological disorder that has been associated with mutations affecting the mitochondrial energy-transduction system [7]. Animals were treated as previously reported [23]. Briefly, pups were weaned and genotyped at ~28 days after birth. All cages were provided with daily food, water, and hydrated gel.

2.2 Brain MRI and proton magnetic resonance spectroscopy (^{1}H MRS)

MRI and ^{1}H MRS experiments were performed on a horizontal 7T-MRI unit (BioSpec 70/30 USR, Bruker Biospin, Ettlingen, Germany). Brain MRI and ^{1}H MRS were performed on the KO ($n=6$) and WT ($n=6$) mice at 6 weeks of age. All MR experiments of the brain were performed with the mice under general anesthesia with isoflurane (2.0% for induction and 1.0% for maintenance for the KO mice, and 3.0% for induction and 2.0% for maintenance for the control mice). During the MR experiments, mice were positioned in a dedicated stereotaxic frame with mouth and ear bars to prevent any movements during MR acquisition. Body temperature was maintained at 36.5 °C with regulated water flow and continuously monitored using a physiological monitoring system (SA Instruments, Inc., Stony Brook, NY, USA). The isoflurane level was adjusted to approximately 1.0% or 2.0% to maintain the respiratory rate in the range of 30–50 breaths per minute.

Anatomical T_2WI performed with a Rapid Acquisition with Refocused Echoes (RARE) sequence (TR/TE = 4000/33 ms, rare factor = 8, field-of-view = 19.2 × 19.2 mm^2, matrix = 256 × 256, in-plane resolution = 75 × 75 μm^2, 10 slices with thickness = 1 m, 4 averages) in transaxial orientation were used for evaluation of brain lesions.

The CEST imaging pulse sequence consisted of a magnetization transfer (MT) RARE sequence modified to saturate a range of frequency offsets. CEST imaging of the mice brains was performed using a RARE readout pulse sequence with a frequency-selective continuous wave saturation preparation pulse. The sequence parameters were as follows: field of view = 19.2 × 19.2 mm^2, slice thickness = 1 mm, TR = 4000 ms, TE = 43 ms, matrix size = 128 × 128, number of averages = 1, in-plane resolution = 150 × 150 μm^2, 1 slice with thickness = 1 mm. The Z-spectra were collected using a 1300-ms saturation pulse at a B_1 amplitude of 3.0 μT with varying frequencies from − 5.0 to + 5.0 ppm (step, 0.5 ppm, 20 images) with one S_0 image (without MT pulse) [16, 18]. A point-by-point B_0 correction was performed from − 1.0 to + 1.0 ppm (step, 0.1 ppm, 20 images) with a B_0 map using a technique referred to as water saturation shift referencing (WASSR) [24]. A total of 41 images including B_0 mapping were acquired in approximately 35 min. The magnetization transfer ratio (MTR) asymmetry was calculated as described in a previous report [25]. The MTR asymmetry curves were obtained from the CEST image series. Five MTR asymmetry maps at 0.5, 1.0, 2.0, 3.0, and 3.5 ppm (amide proton transfer [APT] imaging) were reconstructed using the 41 CEST images.

For MRS, T_2W images were used for accurately positioning a voxel of 2 × 2 × 2 mm^3 in both cortices. The homogeneity of the magnetic field was obtained using a fast, automated shimming technique by mapping along projections (FASTMAP) sequence; good shimming was achieved in the voxel (between 6.8 and 10.8 Hz). ^{1}H MRS acquisition was performed using a PRESS (point resolved spectroscopy) sequence [TR/TE = 2500/20 ms combined with variable power RF pulses with optimized relaxation delays (VAPOR) water suppression]. Metabolite spectra were acquired using 256 repetitions with VAPOR and 32 repetitions without VAPOR for a total scan time of 12 min. Metabolite concentrations, including those of myoinositol (mIns), lactate (lac), glycerophosphocholine + phosphocholine (GPC + PCh), N-acetylaspartate + N-acetylaspartylglutamate (NAA + NAAG), creatine (Cr), and glutamate + glutamine (Glu + Gln) were quantified using the basis set of LCModel [26].

2.3 Statistical analysis

The MTR asymmetry and metabolite concentrations are expressed as mean values ± standard deviations (SD). Intergroup differences were analyzed by the unpaired t-test using Prism 5 (Version 5, GraphPad Software, CA, USA). A p value of < 0.05 was considered statistically significant.

3 Results

Representative T_2WI axial images at the olfactory bulb, cortex, hippocampus, cerebellum, and brain stem levels are shown in Fig. 1. T_2WI MRI revealed no obvious abnormal findings at these regions of the KO (Fig. 1a–c) or WT mice (Fig. 1d–f) at 6 weeks of age.

Typical MTR asymmetry maps at five offset frequencies are shown in Fig. 2. The MTR asymmetry maps at 0.5 ppm, 1.0 ppm, and 2.0 ppm in the KO mice (Fig. 2a–c) were higher than those in the control WT mice (Fig. 2f–h). There were no differences between the MTR asymmetry maps at 3.0 ppm and 3.5 ppm in the KO mice (Fig. 2d, e) or those for the control WT mice (Fig. 2i, j). The Z-spectra and MTR asymmetry curves for the KO and WT groups are shown in Fig. 3A, B. The MTR asymmetry curve of the KO group was higher than that of the control group (Fig. 3b). The quantitative values of MTR asymmetry for the KO mice brains were higher than those for the control mice brains at 0.5 ppm (Fig. 4a, $p < 0.001$), 1.0 ppm (Fig. 4b, $p < 0.001$), and 2.0 ppm (Fig. 4c, $p < 0.001$). However, there were no differences in the quantitative values of MTR asymmetry between the KO and WT mice at 3.0 ppm (Fig. 4d) and 3.5 ppm (Fig. 4e).

Representative MRS spectra are shown in Fig. 5a, b. Brain ^{1}H MRS revealed a significant lactate peak in all KO

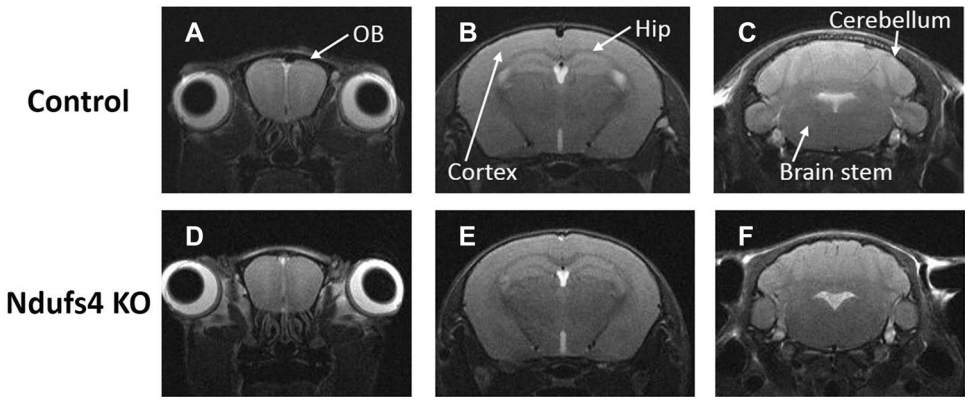

Fig. 1 Representative T_2WI of KO and WT mice brains. White arrows indicate olfactory bulb (OB), cortex, hippocampus (Hip), cerebellum, and brain stem in T_2WI. T_2W MRI revealed no obvious abnormal findings at these regions in the KO or WT mice

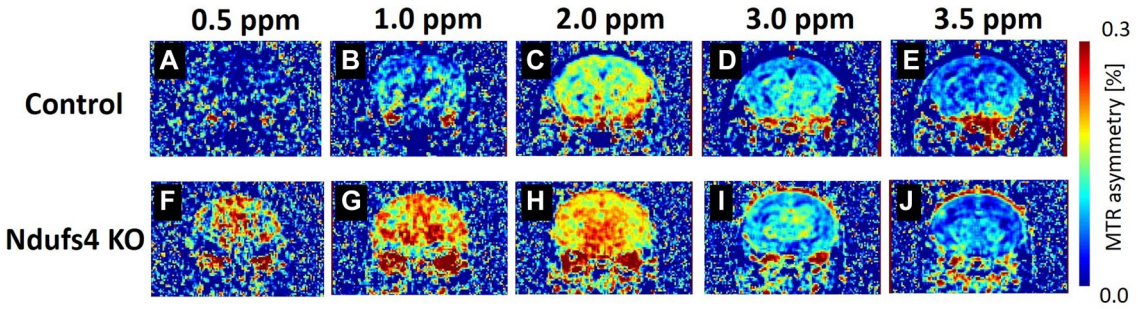

Fig. 2 Representative MTR maps of mice brains. Typical MTR asymmetry maps at five offset frequencies. The MTR asymmetry maps at 0.5 ppm, 1.0 ppm, and 2.0 ppm in KO mice were higher than those in the control WT mice. There were no differences of the MTR asymmetry maps at 3.0 ppm and 3.5 ppm between the KO mice and control WT mice. *KO* knockout, *MTR* magnetization transfer ration, *WT* wild-type

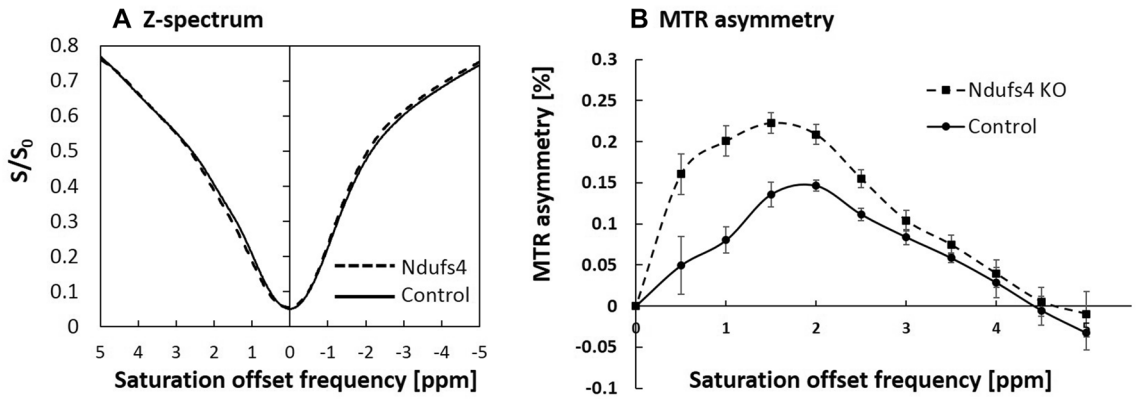

Fig. 3 MTR asymmetry curves. **a** The cumulative curves of Z-spectrum for the KO and Wt mice. **b** The cumulative curves of MTR asymmetry for the KO and Wt mice. The MTR asymmetry curve of the KO group is higher than that of the control group. *KO* knockout, *MTR* magnetization transfer ration, *WT* wild-type

mice (Fig. 5b) compared to that in the control mice (Fig. 5a). Quantitative evaluation of ^{1}H MRS metabolites are shown in Fig. 6a–f. In the KO mice, the lactate levels were significantly higher than those in the control mice (7.2 ± 1.4 mM vs. 3.4 ± 0.6 mM, $p < 0.001$), as shown in Fig. 6b. The creatine levels in the KO mice were slightly higher than those in the control mice (6.9 ± 0.5 mM vs. 6.4 ± 0.3 mM, $p < 0.05$, Fig. 6e). However, the levels of the other five metabolites, including mIns, (4.8 ± 0.5 mM vs. 5.2 ± 0.3 mM, Fig. 6a), GPC + PCh (1.7 ± 0.4 mM vs. 1.7 ± 0.1 mM, Fig. 6c), NAA + NAAG (5.5 ± 0.4 mM vs. 5.2 ± 0.5 mM, Fig. 6d), and Glu + Gln (11.4 ± 1.1 mM vs. 11.6 ± 1.5 mM, Fig. 6f) were not significantly different.

4 Discussion

This is the first report to demonstrate the early detection of intracerebral elevated lactate levels in a mouse model of Leigh syndrome with CEST and ^{1}H MRS. For the CEST evaluation, MTR asymmetry in the KO mice brains was higher than that in the control mice brains at the lower ppm levels (0.5–2.0 ppm), while there was no difference in MTR between the KO and WT mice at the higher ppm levels (3.0–3.5 ppm). Using MRS, we observed increased intracerebral lactate levels before the detection of brain lesions. In addition, the creatine levels in the KO mice

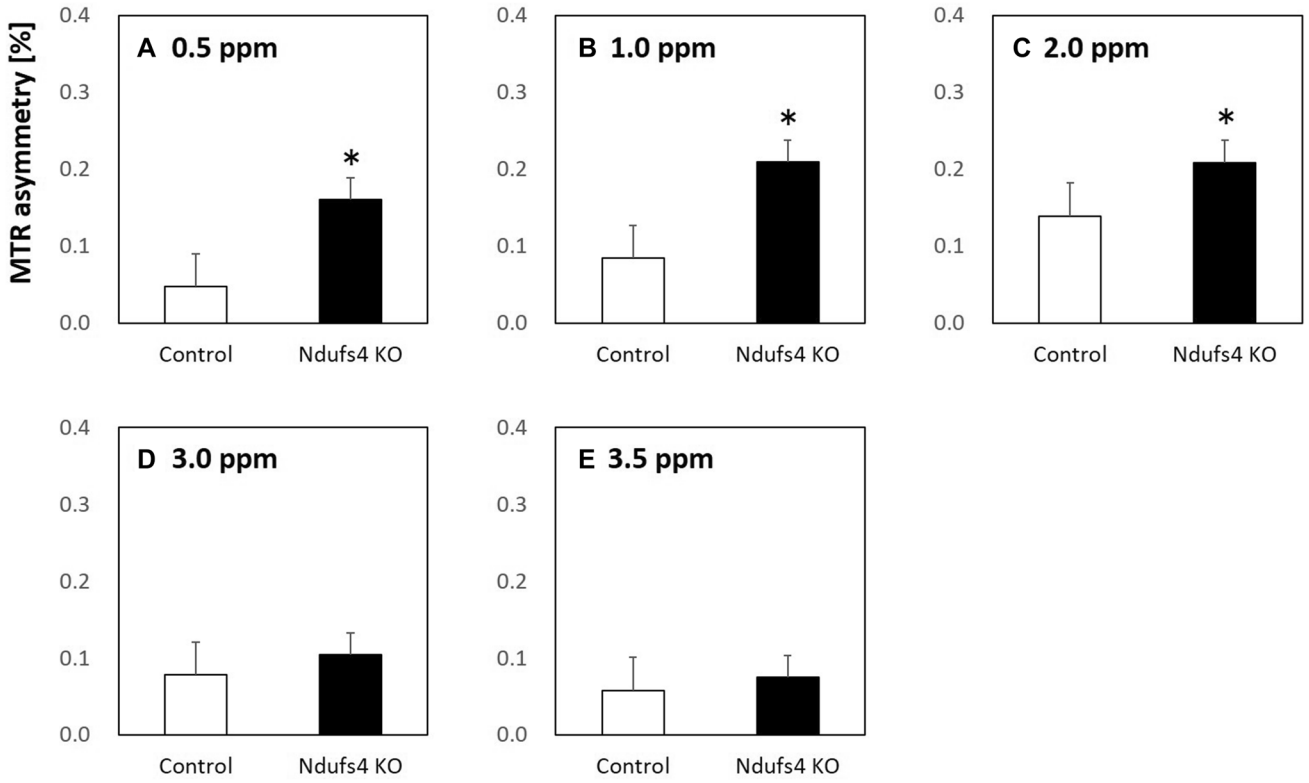

Fig. 4 Representative MTR curves. MTR asymmetry of the KO mice are higher compared with that of the control mice brains at 0.5 ppm (**a**, $p < 0.001$), 1.0 ppm (**b**, $p < 0.001$) and 2.0 ppm (**c**, $p < 0.001$). There are no differences in MTR asymmetry between the KO and Wt mice at 3.0 ppm (**d**) or 3.5 ppm (**e**). *KO* knockout, *MTR* magnetization transfer ration, *WT* wild-type

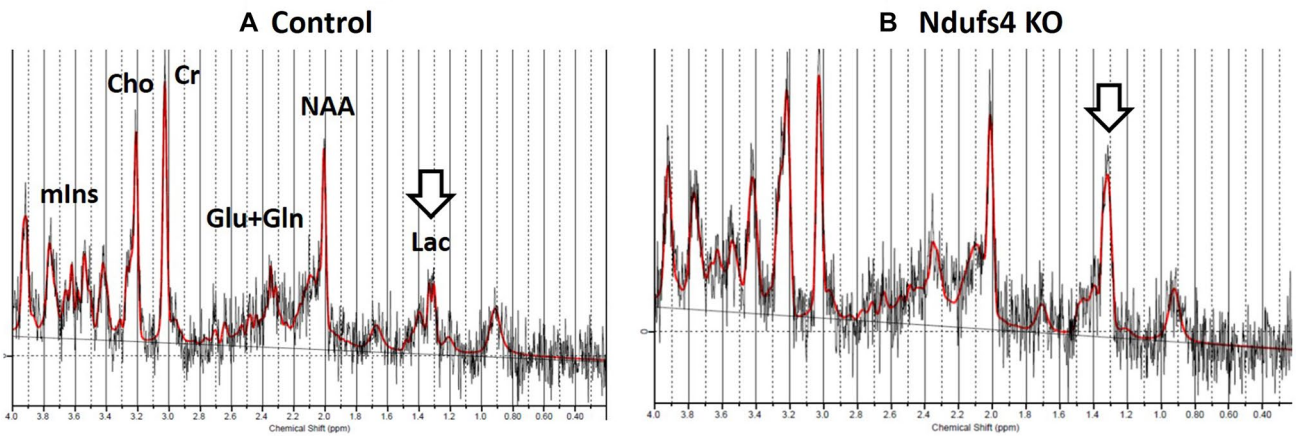

Fig. 5 Representative spectra of ^{1}H MRS. **a** An image from the control mice with no significant lactate peak (arrow). **b** An image from the KO mice with an elevated lactate peak (arrow). The red curve represents the fitted spectrum using LC model. *KO* knockout, *^{1}H MRS* proton magnetic resonance spectroscopy

were slightly higher than those in the control mice. The levels of other metabolites such as mIns, GPC + PCh, NAA + NAAG, and Glu + Gln did not change in the *Ndufs4* KO mitochondrial disease mice. These findings suggest that the CEST effects from 0.5 to 1.0 ppm were detected as an alteration in the lactate levels in the brains of the KO mice. Moreover, there is a possibility that the CEST effect at around 2.0 ppm was detected as an alteration in the Cr level in the KO mice brains. In our results, the intracerebral lactate levels evaluated by CEST and MRS reflected

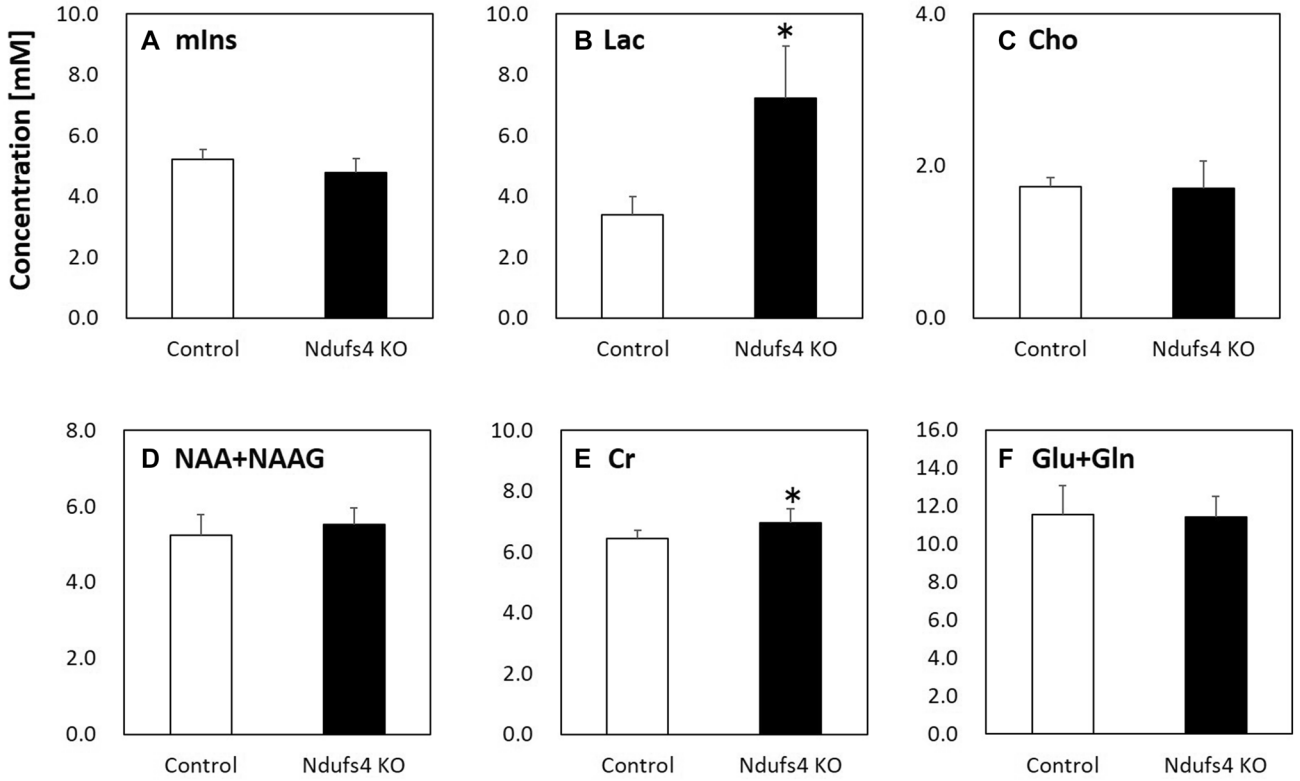

Fig. 6 The lactate levels qualified by LC model in the control and KO mice. The lactate levels in the KO mice were significantly higher than those in the control mice (7.2 ± 1.4 mM vs. 3.4 ± 0.6 mM, $p < 0.001$, **b**). The creatinine kevels in KO mice were slightly higher than those in the control mice (6.9 ± 0.5 mM vs. 6.4 ± 0.6 mM, $p < 0.05$, **e**). The other four metabolites, including mIns (**a**), GPC + PCh (**c**), NAA + NAAG (**d**), and Glu + Gln (**f**) did not change significantly in the KO mice. *KO* knockout

mitochondrial disease progression before the development of brain lesions.

The homozygous *Ndufs4*-KO mice is an established Leigh syndrome mouse model [19–22]. In a previous report, serial T_2WI MRI revealed no obvious abnormal findings in KO mice before 7 weeks of age; only KO mice aged 9 weeks showed bilateral and symmetrical lesions in the postlateral portion of the olfactory bulb and brainstem [21]. T_2WI MRI revealed no obvious abnormal findings at these regions of the KO and WT mice at 6 weeks of age in this study. The KO mice used in this study represented an early stage of the mitochondrial disease model, before the detection of brain lesions was possible.

The CEST effects from 0.5 to 1.0 ppm were detected as an alteration of lactate levels in the brains of 6-week-old KO mice in this study. Lactate was detected as the chemical shift of hydroxyl protons that varies from 0.4 to 0.8 ppm as the temperature changed from 27 to 40 °C [18]. In addition, the CEST signal from lactate may be affected by the pH in different subjects. This suggests that the CEST signals at 0.5 ppm and 1.0 ppm reflected elevated intracerebral lactate levels in the mitochondrial disease models. Mitochondrial disease patients show a significant intracerebral lactate peak and an association with the intracerebral lactate levels [10–12, 19, 27–30]. There are several serum biomarkers of mitochondrial disease [22, 31, 32]; however, in comparison with the other serum biomarkers, intracerebral lactate is expected to be a useful mitochondrial disease biomarker. Therefore, non-invasive imaging of the lactate biomarker using CEST and MRS is useful for evaluation of mitochondrial disease. Moreover, CEST can be evaluated with brain mapping, though MRS has disadvantages due to its poor spatial resolution. Mapping the spatial distribution of nuclei associated with a particular chemical shift using MRS is called chemical shift imaging (CSI). CSI is a multi-voxel technique that utilizes phase-encoding, in whole or part, for spatial localization. The major disadvantages of CSI include longer set-up and imaging time, difficulty in obtaining a homogenous shim over the entire region, and lower signal-to-noise and spectral quality for individual voxels.

When developing a CEST biomolecule evaluation method in vivo, it is necessary to consider other possible contributions to the CEST signal from amide, amine, and hydroxyl protons associated with other metabolites and nuclear Overhauser enhancement (NOE) [33]. The chemical shift of hydroxyl protons of mIns has been observed

at around 0.6 ppm [34]. The metabolite of mIns, located mainly in glial cells, is one of the most abundant metabolites in the brain and functions as an osmolyte. The concentration of mIns is altered in brain-degenerative diseases such as Alzheimer's disease [34, 35]. However, there was no change in mIns in MRS evaluations in the homozygous *Ndufs4* KO mice (Leigh syndrome mouse models) in our study. This suggests that the contribution to 0.5 ppm CEST signal from mIns is smaller than that from lactate.

Creatine CEST contrast was computed by subtracting the normalized magnetization signal at the creatine proton frequency of around + 1.8 ~ 2.0 ppm from the magnetization at the corresponding reference frequency on the opposite side of the water resonance [19, 27]. The creatine CEST can detect changes in muscle creatine content after exercise in individuals with mitochondrial disorders [19]. In addition, some studies investigated that creatine could be used as a biomarker for mitochondrial diseases, given its known link with mitochondrial bioenergetics [36]. Plasma creatine levels were higher in patients with some kinds of mitochondrial diseases than in healthy subjects [37]. In our study, MTR asymmetry of the KO mice brains was higher than that of the control mice brains at 2.0 ppm. In the KO mice, the creatine levels evaluated by MRS were slightly higher than those in control mice. This finding suggests that the CEST signal from creatine at around 2.0 ppm was affected by creatine levels in the KO mice. Our results offer the possibility of developing creatine CEST as a potential non-invasive imaging-based biomarker in individuals with diverse types of mitochondrial diseases presenting with symptoms involving the muscle and brain. Moreover, the creatine CEST for mitochondrial diseases may be used for the evaluation of progression and treatment effect. Therefore, creatine CEST needs to be a more accurate and robust method such as the combined 3D and rapid sequences.

MTR asymmetry curves of the KO mice at 3.0 ppm and 3.5 ppm were not significantly different between the two groups in the present study. It has been shown that Glu exhibits a concentration-dependent CEST effect (GluCEST) between its amine and bulk-water protons [15]. In addition, APT is a special type of CEST that shows selective irradiation at 3.5 ppm from water to saturate amide protons [13]. However, several in vivo confounding factors for APT CEST imaging include effects of tissue relaxation, semisolid MT, relayed NOEs from aliphatic protons, and contributions from other nearby exchanging protons such as amines [38–40]. Therefore, it is necessary to carefully consider the effects of NOE on CEST around 3.5 ppm. There was no alteration of Glu in the homozygous *Ndufs4* KO mice. This suggests that the CEST signal from Glu at around 3.0 ppm and APT at around 3.5 ppm did not affect Glu levels or other metabolites in the KO mice.

While there are clear advantages of CEST imaging for lactate in comparison with other methods, there are also some challenges to address. CEST imaging in this study was performed using a single-slice RARE sequence. In a previous report, T_2WI MRI revealed abnormal findings in KO mice at 9 weeks of age; bilateral and symmetrical lesions were detected in the postlateral portion of the olfactory bulb and brainstem [20]. Sun et al. proposed that a fast multi-slice relaxation self-compensated CEST MRI sequence would significantly improve sensitivity [41]. Multi-slice whole brain maps for lactate that include the olfactory bulb and brainstem in mitochondrial disease are needed to investigate the heterogeneities of brain regions. To address this need, a multi-slice CESTMRI acquisition method with CEST is needed in future studies. Moreover, there is a greater effect of direct saturation because the hydroxyl protons of lactate resonate very close to the large water peak. Lactate is the chemical shift of hydroxyl protons varied from 0.4 to 0.8 ppm [17]. In addition, the CEST signal from lactate can be altered by the pH in subjects. The CEST imaging in our study was performed by the WASSR method [23]. Although this method was sufficient for the B_0 correction because we used a single-slice sequence, a robust B_0 correction method is required for multi-slice CEST imaging for lactate.

5 Conclusion

We performed brain CEST and ^{1}H MRS experiments in Leigh syndrome mouse models and detected elevated lactate levels in the KO mice. In addition, we proposed that CEST imaging can be used to evaluate intracerebral elevated lactate levels as a biomarker for mitochondrial disease at 7T-MRI.

Acknowledgements We thank Dr. Rikita Araki (Bruker Biospin) for CEST calculation used in the current study.

Funding This work was supported by Grants-in-Aid for Scientific Research (Kakenhi, No. 16K090170 and 15K21774) from the Japan Society for the Promotion of Science (JSPS).

Compliance with ethical standards

Conflict of interest The authors declare no financial or commercial conflicts of interest.

Ethical approval All applicable international, national, and/or institutional guidelines for the care and use of animals were followed. This article does not contain any studies with human participants performed by any of the authors.

References

1. Gorman GS, Chinnery PF, DiMauro S, Hirano M, Koga Y, McFarland R, Suomalainen A, Thorburn DR, Zeviani M, Turnbull DM. Mitochondrial diseases. Nat Rev Dis Primers. 2016;2:16080.
2. Vafai SB, Mootha VK. Mitochondrial disorders as windows into an ancient organelle. Nature. 2012;491(7424):374–83.
3. Schapira AH. Mitochondrial diseases. Lancet. 2012;379(9828):1825–34.
4. Lake NJ, Bird MJ, Isohanni P, Paetau A. Leigh syndrome: neuropathology and pathogenesis. J Neuropathol Exp Neurol. 2015;74(6):482–92.
5. Lee JS, Kim H, Lim BC, Hwang H, Choi J, Kim KJ, Hwang YS, Chae JH. Leigh syndrome in childhood: neurologic progression and functional outcome. J Clin Neurol. 2016;12(2):181–7.
6. Sofou K, De Coo IF, Isohanni P, Ostergaard E, Naess K, De Meirleir L, Tzoulis C, Uusimaa J, De Angst IB, Lonnqvist T, Pihko H, Mankinen K, Bindoff LA, Tulinius M, Darin N. A multicenter study on Leigh syndrome: disease course and predictors of survival. Orphanet J Rare Dis. 2014;9:52.
7. Lee HF, Tsai CR, Chi CS, Lee HJ, Chen CC. Leigh syndrome: clinical and neuroimaging follow-up. Pediatr Neurol. 2009;40(2):88–93.
8. Torraco A, Diaz F, Vempati UD, Moraes CT. Mouse models of oxidative phosphorylation defects: powerful tools to study the pathobiology of mitochondrial diseases. Biochim Biophys Acta. 2009;1793(1):171–80.
9. Lin DD, Crawford TO, Barker PB. Proton MR spectroscopy in the diagnostic evaluation of suspected mitochondrial disease. AJNR Am J Neuroradiol. 2003;24(1):33–41.
10. Kaufmann P, Shungu DC, Sano MC, Jhung S, Engelstad K, Mitsis E, Mao X, Shanske S, Hirano M, DiMauro S. De Vivo DC. Cerebral lactic acidosis correlates with neurological impairment in MELAS. Neurology. 2004;62(8):1297–302.
11. Boddaert N, Romano S, Funalot B, Rio M, Sarzi E, Lebre AS, Bahi-Buisson N, Valayannopoulos V, Desguerre I, Seidenwurm D, Brunelle F, Brami-Zylberberg F, Rotig A, Munnich A de. Lonlay P. 1H MRS spectroscopy evidence of cerebellar high lactate in mitochondrial respiratory chain deficiency. Mol Genet Metab. 2008;93(1):85–8.
12. Cakmakci H, Pekcevik Y, Yis U, Unalp A, Kurul S. Diagnostic value of proton MR spectroscopy and diffusion-weighted MR imaging in childhood inherited neurometabolic brain diseases and review of the literature. Eur J Radiol. 2010;74(3):e161-71.
13. Ward KM, Aletras AH. Balaban RS. A new class of contrast agents for MRI based on proton chemical exchange dependent saturation transfer (CEST). J Magn Reson. 2000;143(1):79–87.
14. Kogan F, Hariharan H, Reddy R. Chemical exchange saturation transfer (CEST) imaging: description of technique and potential clinical applications. Curr Radiol Rep. 2013;1(2):102–14.
15. Cai K, Haris M, Singh A, Kogan F, Greenberg JH, Hariharan H, Detre JA, Reddy R. Magnetic resonance imaging of glutamate. Nat Med. 2012;18(2):302–6.
16. Saito S, Mori Y, Tanki N, Yoshioka Y, Murase K. Factors affecting the chemical exchange saturation transfer of Creatine as assessed by 11.7 T MRI. Radiol Phys Technol. 2015;8(1):146–52.
17. Cai K, Singh A, Poptani H, Li W, Yang S, Lu Y, Hariharan H, Zhou XJ. Reddy R. CEST signal at 2 ppm (CEST@2 ppm) from Z-spectral fitting correlates with creatine distribution in brain tumor. NMR Biomed. 2015;28(1):1–8.
18. DeBrosse C, Nanga RP, Bagga P, Nath K, Haris M, Marincola F, Schnall MD, Hariharan H, Reddy R. Lactate chemical exchange saturation transfer (LATEST) imaging in vivo A biomarker for LDH activity. Sci Rep. 2016;6:19517.
19. DeBrosse C, Nanga RP, Wilson N, D'Aquilla K, Elliott M, Hariharan H, Yan F, Wade K, Nguyen S, Worsley D, Parris-Skeete C, McCormick E, Xiao R, Cunningham ZZ, Fishbein L, Nathanson KL, Lynch DR, Stallings VA, Yudkoff M, Falk MJ, Reddy R. McCormack SE. Muscle oxidative phosphorylation quantitation using creatine chemical exchange saturation transfer (CrCEST) MRI in mitochondrial disorders. JCI Insight. 2016;1(18):e88207.
20. Kruse SE, Watt WC, Marcinek DJ, Kapur RP, Schenkman KA, Palmiter RD. Mice with mitochondrial complex I deficiency develop a fatal encephalomyopathy. Cell Metab. 2008;7(4):312–20.
21. Quintana A, Kruse SE, Kapur RP, Sanz E, Palmiter RD. Complex I deficiency due to loss of Ndufs4 in the brain results in progressive encephalopathy resembling Leigh syndrome. Proc Natl Acad Sci USA. 2010;107(24):10996–1001.
22. Jain IH, Zazzeron L, Goli R, Alexa K, Schatzman-Bone S, Dhillon H, Goldberger O, Peng J, Shalem O, Sanjana NE, Zhang F, Goessling W, Zapol WM. Mootha VK. Hypoxia as a therapy for mitochondrial disease. Science. 2016;352(6281):54–61.
23. Ferrari M, Jain IH, Goldberger O, Rezoagli E, Thoonen R, Cheng KH, Sosnovik DE, Scherrer-Crosbie M, Mootha VK. Zapol WM. Hypoxia treatment reverses neurodegenerative disease in a mouse model of Leigh syndrome. Proc Natl Acad Sci USA. 2017;114(21):E4241-E50.
24. Kim M, Gillen J, Landman BA, Zhou J, van Zijl PC. Water saturation shift referencing (WASSR) for chemical exchange saturation transfer (CEST) experiments. Magn Reson Med. 2009;61(6):1441–50.
25. Liu G, Gilad AA, Bulte JW, van Zijl PC, McMahon MT. High-throughput screening of chemical exchange saturation transfer MR contrast agents. Contrast Media Mol Imaging. 2010;5(3):162–70.
26. Provencher SW. Estimation of metabolite concentrations from localized in vivo proton NMR spectra. Magn Reson Med. 1993;30(6):672–9.
27. Haris M, Singh A, Cai K, Kogan F, McGarvey J, Debrosse C, Zsido GA, Witschey WR, Koomalsingh K, Pilla JJ, Chirinos JA, Ferrari VA, Gorman JH, Hariharan H, Gorman RC, Reddy R. A technique for in vivo mapping of myocardial creatine kinase metabolism. Nat Med. 2014;20(2):209–14.
28. Chi CS, Lee HF, Tsai CR, Chen WS, Tung JN, Hung HC. Lactate peak on brain MRS in children with syndromic mitochondrial diseases. J Chin Med Assoc. 2011;74(7):305–9.
29. Lindroos MM, Borra RJ, Parkkola R, Virtanen SM, Lepomaki V, Bucci M, Virta JR, Rinne JO, Nuutila P, Majamaa K. Cerebral oxygen and glucose metabolism in patients with mitochondrial m.3243A> G mutation. Brain. 2009;132(Pt 12):3274–84.
30. Kaufmann P, Engelstad K, Wei Y, Kulikova R, Oskoui M, Sproule DM, Battista V, Koenigsberger DY, Pascual JM, Shanske S, Sano M, Mao X, Hirano M, Shungu DC, Dimauro S, De Vivo DC. Natural history of MELAS associated with mitochondrial DNA m.3243A> G genotype. Neurology. 2011;77(22):1965–71.
31. Thompson Legault J, Strittmatter L, Tardif J, Sharma R, Tremblay-Vaillancourt V, Aubut C, Boucher G, Clish CB, Cyr D, Daneault C, Waters PJ, Consortium L, Vachon L, Morin C, Laprise C, Rioux JD, Mootha VK. Des Rosiers C. A metabolic signature of mitochondrial dysfunction revealed through a monogenic form of leigh syndrome. Cell Rep. 2015;13(5):981–9.
32. Steele HE, Horvath R, Lyon JJ. Chinnery PF. Monitoring clinical progression with mitochondrial disease biomarkers. Brain. 2017;140(10):2530–40.
33. Jin T, Wang P, Zong X, Kim SG. MR imaging of the amide-proton transfer effect and the pH-insensitive nuclear overhauser effect at 9.4 T. Magn Reson Med. 2013;69(3):760–70.
34. Haris M, Cai K, Singh A, Hariharan H, Reddy R. In vivo mapping of brain myo-inositol. Neuroimage. 2011;54(3):2079–85.

35. Chen SQ, Wang PJ, Ten GJ, Zhan W, Li MH, Zang FC. Role of myo-inositol by magnetic resonance spectroscopy in early diagnosis of Alzheimer's disease in APP/PS1 transgenic mice. Dement Geriatr Cogn Disord. 2009;28(6):558–66.
36. Wallimann T, Dolder M, Schlattner U, Eder M, Hornemann T, O'Gorman E, Ruck A, Brdiczka D. Some new aspects of creatine kinase (CK): compartmentation, structure, function and regulation for cellular and mitochondrial bioenergetics and physiology. Biofactors. 1998;8(3–4):229–34.
37. Pajares S, Arias A, Garcia-Villoria J, Briones P, Ribes A. Role of creatine as biomarker of mitochondrial diseases. Mol Genet Metab. 2013;108(2):119–24.
38. Zu Z, Janve VA, Li K, Does MD, Gore JC, Gochberg DF. Multi-angle ratiometric approach to measure chemical exchange in amide proton transfer imaging. Magn Reson Med. 2012;68(3):711–9.
39. Zhang XY, Wang F, Afzal A, Xu J, Gore JC, Gochberg DF. Zu Z. A new NOE-mediated MT signal at around – 1.6 ppm for detecting ischemic stroke in rat brain. Magn Reson Imaging. 2016;34(8):1100–6.
40. Zhang XY, Wang F, Jin T, Xu J, Xie J, Gochberg DF, Gore JC. Zu Z. MR imaging of a novel NOE-mediated magnetization transfer with water in rat brain at 9.4 T. Magn Reson Med. 2017;78(2):588–97.
41. Sun PZ, Cheung JS, Wang E, Benner T, Sorensen AG. Fast multi-slice pH-weighted chemical exchange saturation transfer (CEST) MRI with Unevenly segmented RF irradiation. Magn Reson Med. 2011;65(2):588–94.